



Removal of Congo red by magnetic nano-alumina using response surface methodology and artificial neural network

Sadrollah Hassani^a, Mahboube Shirani^a, Abolfazl Semnani^{a,*}, Mohsen Hassani^b, Alireza Firooz^c

^aDepartment of Chemistry, Faculty of Science, Shahrekord University, Shahrekord, P.O. Box 115, Iran, Tel. +98-381-4424419; Fax: +98-381-4424419; email: a.semnani1341@gmail.com

^bDepartment of Mechanical Engineering, Najafabad Branch, Islamic Azad University, Isfahan, Iran

^cDepartment of Chemistry, University of Isfahan, 8818634141, Isfahan, Iran

Received 6 January 2016; Accepted 9 June 2016

ABSTRACT

Easily separable magnetic nano alumina was synthesized for the removal of the toxic dye Congo red from aqueous solution. Magnetic nano alumina particles were characterized by SEM-EDX. The magnetic property of the sorbent was evaluated by the VSM method. The obtained saturation magnetization of 15.88 emu g⁻¹ showed facile separation of magnetic nano alumina. The effect of influential parameters; pH, temperature, time, initial dye concentration and amount of sorbent on the removal (%) were investigated. The removal (%) was mathematically described as a function of experimental parameters and central composite design (CCD) was applied to estimate the process. The same design was used for a three layer artificial neural network (ANN) model. The predicted CCD data vs. ANN showed a regression value of 0.9999. This linear agreement indicated that the CCD and ANN could ideally predict the process. The results of the two models were compared in terms of coefficient of determination and mean absolute percentage error to indicate the prediction potential of CCD and ANN. The obtained results confirm higher capability and accuracy of ANN in prediction compared with CCD. The experimental data were found to be properly fitted to the Langmuir and Freundlich model which indicates that the sorption takes place on a heterogeneous material. A sorption capacity of 27.397 (mg g⁻¹) was achieved for Congo red.

Keywords: Removal; Congo red; Magnetic nano-alumina; Statistical modeling; Artificial neural network; Central composite design

1. Introduction

Dyes are widely utilized in textile, printing, cosmetic and food industries. Most of these dyes are toxic and releasing them into water sources such as rivers, lakes and seas has been a serious concern due to the water pollution and aquatic living organism death. Water pollution is one of the most considerable factors of human health. Aggregation of dyes in water causes cancer, genetic mutation, digestive disorders and poisoning. Congo red is one of most widespread anionic dyes used in all dye industries to provide red color. Congo

red accumulation in human body can cause cancer, severe allergic reaction and acute inhalation [1, 2]. Separation and removal of Congo red from water sources is environmentally important. Various techniques such as oxidative degradation [3], coagulation [4], membrane filtration [5], ozonation [6] and adsorption [7–9] were reported for toxic dyes removal from aqueous solutions. However, among all removal techniques, adsorption is much more common due to the advantages of simplicity, low cost adsorbents, easy industrialization, and facile accessibility. Zeolite [10], active carbon [11] and alumina are widely used for removal of different dyes. Alumina is a prevalent sorbent which is extensively used for adsorption of different contamination [12–14]. Magnetic sorbents have

* Corresponding author.

been introduced for adsorption techniques in last decades which make the separation of sorbent much easier from media and overcome the dispersion of the sorbent after adsorption process [15–17]. Nano structure materials have some significant properties such as larger surface area than bulk particles which increase their application in adsorption process [18]. No study has been reported for applying magnetic nano alumina for dye removal. In this study, Congo red, as an anionic dye, was adsorbed by magnetic nano alumina from aqueous solution.

In recent years, statistical models have been introduced to simulate different systems. Artificial neural network (ANN) and response surface methodology (RSM) are the most prevalent models which can ideally predict chemical processes [19]. ANN is an advanced prediction model which is initially acquired from the neurons function in human brain [20]. ANN overcomes the drawbacks of most mathematical models due to ANN ability in application in both linear and non-linear systems [21–24]. ANN can effectively predict complex nonlinear relationships between parameters and prediction of output variables. ANN has been reported for adsorption of Congo red [25]. RSM deals with a group of mathematical and statistical techniques to fit predicted model to the experimental data. RSM is a powerful method for prediction of large number of processes which is applied in two common designs of Box–Behnken design (BBD) and central composite design (CCD) [26]. Adsorption of Congo red onto cashew nut shell using RSM was reported previously [27]. In this study, removal of Congo red by magnetic nano alumina from aqueous solutions was investigated. The process was considered applying two potent statistical models of RSM and ANN and the coefficient of determination (R^2) and mean absolute percentage error (MAPE) of RSM and ANN were compared.

2. Materials and method

2.1. Materials

Congo red ($C_{32}H_{22}N_6Na_2O_6S_2$) (Dye content $\geq 35\%$) was purchased from Sigma Aldrich (Kimia-ExirCo. in Tehran, Iran.). Hydrochloric acid, sodium hydroxide which applied for both magnetization and setting the acidity and basicity of the solution, were purchased from Merck. Iron (II) chloride tetrahydrate ($\geq 99.0\%$), iron (III) chloride hexahydrate ($\geq 98\%$) were used for preparation of magnetic alumina. Nano alumina (<50 nm particle size) was purchased from Sigma-Aldrich. All chemicals used in this study were analytical grade with the highest purity available and they were purchased from Merck and Sigma-Aldrich.

2.2. Apparatus

The pH adjustment in the process was done by 86502-pH/ORP (AZ Instrument, Taiwan) using a combined glass calomel electrode. Magnetic nano alumina was prepared using Ultrasonic bath (Sonorex Digitec, DT255H, Germany) and oven (Universal model UF 55, Germany). IKA overhead stirrer (model RW 28 digital Package, Germany) with glass stirrer was utilized to stir the magnetic sorbent sample solution during adsorption process. Ultrospect 3100 pro UV-visible Spectrophotometer (Amersham Biosciences, USA) was employed for data analyzing. In order to characterize the

magnetic properties of synthesized magnetic nano alumina, the vibration–sample magnetometer (Meghnatis Daghigh Kavir Co., Kashan, Iran) was utilized.

2.3. Preparation of magnetic nano alumina

Magnetic nano alumina was prepared according to the proposed procedure [28]. In brief, the mixture of nano alumina in 100 mL of ammonia solution (1 M) was deoxygenated (solution A). The solution of $FeCl_3 \cdot 6H_2O$ (1M) and $FeCl_2 \cdot 4H_2O$ (2 M in HCl 2 M) was deoxygenated too (solution B). Then, the two solutions of A and B were blended under nitrogen atmosphere by ultrasonic treatment. To neutralize the sorbent, it was washed with oxygen free deionized water for several times. Finally, the obtained magnetic nano alumina was dried at $50^\circ C$ in the oven.

2.4. Determination of isoelectric point

The isoelectric point (pH_{IEP}) or point of zero charge (pH_{pzc}) is an indicative factor for linear range of pH sensitivity which represents the type of surface active centers and the adsorption ability of the surface [29, 30]. To determine the pH_{pzc} , the pH of eight dye solutions were set in the range of 4–11 and 15 mg of sorbent was added to each solution [31]. Then, the solutions were shaken separately and let them to achieve to the equilibrium state for 24 h. the final pH of the solutions were determined after the specific time. The pH_{pzc} of 8 was obtained by the plot initial pH vs. final pH of the solution.

2.5. Adsorption procedure

10 mL Congo red solution was adjusted at the CCD experimental design estimated values of parameters (i.e., pH, temperature, time, initial dye concentration, and amount of magnetic nano alumina). Then, the magnetic nano alumina was separated from the aqueous solution by an external magnet and the upper aqueous phase was determined by UV-Visible spectrophotometer.

The uptake of adsorbate can be expressed as follows: [32]

$$Q_i = (C_i - C_e) / S \quad (1)$$

where Q_i is the adsorbate concentration adsorbed at the equilibrium condition (mg of adsorbate/g of adsorbent); C_i is the initial dye concentration in the solution ($mg L^{-1}$); C_e is Equilibrium concentration or final dye concentration ($mg L^{-1}$); S is Dosage concentration which is obtained as following Eq. (2):

$$S = m/v \quad (2)$$

where m is the adsorbent mass (g) and v is the volume of adsorbate solution (L).

Finally the percentage of adsorption percentage can be stated according to the following equation:

$$\text{Adsorption percentage (\%)} = (C_i - C_e) / C_i \times 100 \quad (3)$$

3. Experimental design models

3.1. Response surface methodology

RSM is one of the factorial designs for statistical analysis. RSM is a mathematical and statistical method which is based on the fit of empirical models to the experimental data obtained from experimental design [26, 33]. RSM consists of two designs of CCD and BBD. CCD and BBD are successfully applied in dye removal techniques [34–36]. The optimization of adsorption process was carried out using experimental design of CCD as a partial factorial design. The experimental design was done by MINITAB software version 16.0 to optimize the influential factors of pH, temperature, time, initial dye concentration and amount of sorbent on dye adsorption. Table 1 shows different variables, the symbols and levels.

The precision of the process was evaluated by the three replicates at the center of the design. In order to depict the interaction of the factors in the process, a full quadratic equation was used as follows:

$$Y = b_0 + \sum_{i=1}^k b_i x_i + \sum_{i=1}^k b_{ii} x_i^2 + \sum_{i < j}^{i,j} b_{ij} x_i x_j \tag{4}$$

where Y is the estimated response and b_0, b_i, b_{ii} and b_{ij} are the regression coefficients for the intercept, linearity, square and interaction terms, respectively, and x_i and x_j are the coded independent variables.

3.2. ANN

In the present study, Neural Network Toolbox Version 6.0.4 of MATLAB® R2010, mathematical software, was applied to predict the process. A three-layer ANN with tan-sigmoid and purline function was used for hidden and output layers as transfer functions respectively. A sigmoid function is a bounded differentiable real function that is defined for all real input values and has a positive derivative at each point [37]. The tan-sigmoid transfer function is stated as follows [38]:

$$F(x) = 1 / (1 + \exp(-x)) \tag{5}$$

In the applied ANN, feed forward back propagation (FFBP) was used as training algorithm. Generally, for FFBP, the final calculated outputs are compared with the experimentally obtained outputs, and the errors are calculated.

Table 1
Coded setting and experimental range of variables for removal of Congo red according to the central composite design

Variables	Symbols	Ranges and levels				
		-2	-1	0	+1	+2
pH	x_1	5.5	6.5	7.5	8.5	9.5
Time (min)	x_2	5	15	25	35	45
Temperature (°C)	x_3	25	35	45	55	65
Initial dye concentration (mg L ⁻¹)	x_4	10	20	30	40	50
Amount of sorbent (mg)	x_5	15	25	35	45	55

These errors are then propagated backwards and used for adjusting the weights of neurons. Training network is considered as the process of using the experimental outputs to minimize the mean squared error. The weights of the trained network are stored, and can be applied later for predicting the outputs of a different set of inputs. The obtained experimental data predicted by CCD were considered by ANN. Thirty-two experimental points were used to feed the model, and then 26 and 6 data points as training and test sets were applied, respectively, for data set deriving. Normalization of data points was carried out using tan-sigmoid transfer function in the range of [-0.9, 0.9] as follows:

$$X_{norm} = 1.8 (X - X_{min}) / (X_{max} - X_{min}) - 0.9 \tag{6}$$

where X is variable, X_{min}, X_{max} are minimum and maximum values, respectively.

4. Results and discussion

4.1. Characterization of magnetic nano alumina

The nano structure of the magnetic nano alumina was considered by the SEM image (Fig. 1). The chemical composition of magnetic nano alumina, containing Al (%) of 29.11, O (%) of 50.84 and Fe (%) of 20.05 were achieved by EDX (Fig. 2 and Table 2). The magnetic properties of the

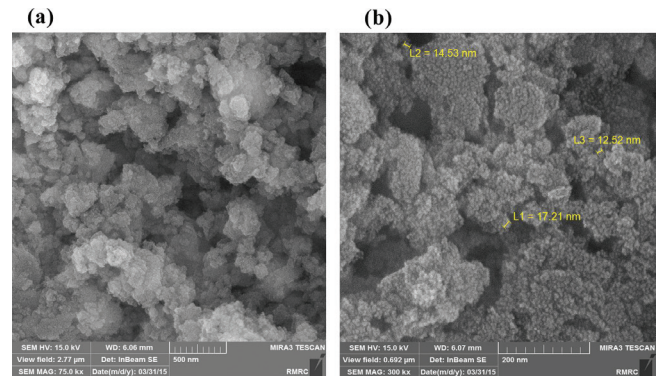


Fig. 1. The SEM image of magnetic nano alumina: (a) 500 nm scale, (b) 200 nm.

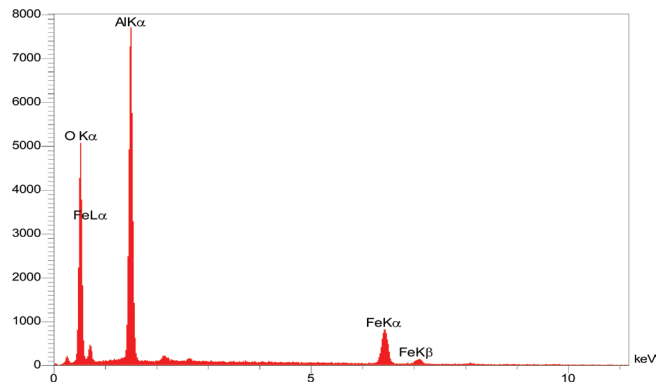


Fig. 2. The EDX image of magnetic nano alumina.

Table 2
The chemical composition of magnetic zeolite obtained by EDX

Element	W% (weight percent)
O	50.84
Al	29.11
Fe	20.05
Total	100.00

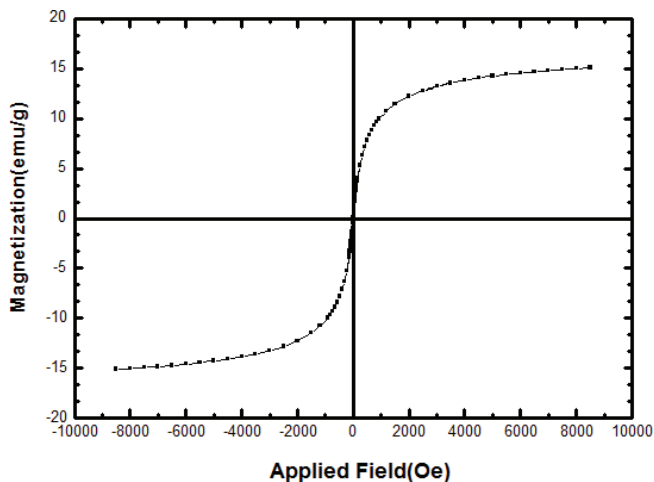


Fig. 3. The hysteresis loops of magnetic nano alumina.

magnetic nano alumina was confirmed by the VSM analysis (Vibrating Sample Magnetometer). The magnetic curve in Fig. 3 shows appropriate super paramagnetic property of magnetic nano alumina due to no hysteresis loop and no eminence existence. While the magnetic nano alumina was exposed to an external magnetic field, it reserves no magnetization and redisposed after magnetic field removal. The saturation magnetization of 15.88 emu g^{-1} at 298 K was observed which proved the attraction of magnetic nano alumina by an external magnet.

4.2. CCD Modeling

The adsorption percent of Congo red as a function of the independent variables within the region of investigation (i.e., aqueous solution) is expressed by Eq. (7):

$$\begin{aligned}
 Y = & 70.751 + 0.329 x_1 + 1.579 x_2 - 2.437 x_3 + 0.479 x_4 + 7.237 x_5 \\
 & - 5.76364 x_1^2 - 2.56364 x_2^2 + 4.17386 x_3^2 - 2.45114 x_4^2 \\
 & - 0.463636 x_5^2 + 2.93125 x_1 x_2 - 5.80625 x_1 x_3 - 4.28125 x_1 x_4 \\
 & + 1.74375 x_1 x_5 - 5.33125 x_2 x_3 - 0.406250 x_2 x_4 + 3.56875 x_2 x_5 \\
 & - 1.79375 x_3 x_5 + 2.48125 x_4 x_5
 \end{aligned}
 \quad (7)$$

Maximum adsorption percent of 99.50% was achieved under the optimum predicted conditions of pH of 7.12, temperature of 25°C , time of 22.03 min, initial dye

concentration of 16.43 mg L^{-1} , and magnetic nano alumina amount of 48.47 mg. The experimental data were analyzed by response surface design (RSD) using the Minitab software. Table 3 shows the MINITAB predicted and experimental responses for 32 runs by CCD model of Congo red adsorption. The results of the statistical analysis including, the estimated regression coefficients and p-values are tabulated in Table 4. The p-values for all variables in the model are all <0.05 , which indicate that the applied model is successfully made an ideal prediction for the process with a linear relationship between the variables. The p-values for all variables in the model which are >0.05 , indicate the non-linear relationship between the interest variables; therefore, these variables would be omitted from the proposed equation for the process. In each run, the predicted results were calculated by substituting the coefficients and numerical values of the variables in Eq. (7). The linear regression coefficients (R^2) of 0.9995 for the predicted data vs. experimental data proved good agreements between predicted and experimental responses. The adjusted R^2 were 99.90%, which reveal the ability of the developed model to predict the percent of dye adsorption in the proposed process.

4.3. Effect of variables on dye removal

The influence of five parameters of pH, temperature, time, initial dye concentration and amount of magnetic nano alumina on dye adsorption and their interactions were studied. The obtained results from CCD prediction are shown in Fig. 4.

4.3.1. The effect of pH

Considering the nature of cationic or anionic dyes, acidity or basicity of the solution is a key factor in the process. Therefore, the pH of the sample solution was considered in the range of 4.5–10.5, using hydrochloride acid and sodium hydroxide. Fig. 4(a)–(d) show that as the pH solution increased to 7.12, the removal (%) increased and then pH decreased up to 7.12. Therefore, the optimum pH of 7.12 was chosen for the process. It seems that at basic conditions (high pH), the surface of the adsorbent becomes negatively charged by hydroxide ions which reduces the electrostatic interaction and the attraction of anionic dye (Congo red) on the negative surface of the adsorbent [39, 40]. At low pH, the surface of sorbent is positively charged which intensifies the Congo red adsorption on the surface. Moreover, the optimum pH was lower than pH_{pzc} which was expected for anionic dyes ($\text{pH} < \text{pH}_{\text{pzc}}$) [41].

4.3.2. The effect of temperature

Generally, in all adsorption processes, temperature plays an important role. The type of dye (cationic or anionic dyes) can provide exothermic or endothermic system [30]. In an endothermic system, as the temperature increases, the percent of adsorption increases due to the adsorption capacity enhancement. Interestingly, the adsorption of anionic dyes is exothermic. Since Congo red is an anionic dye, this statement came true for it. In an exothermic system, the mechanism is

Table 3
Experimental matrix for five-level-five factors CCD for removal of Congo red

Exp. No.	Factors						Removal (%)	
	pH	Temperature (°C)	Time (min)	Initial dye con. (mg L ⁻¹)	M.A. amount (mg)	Obtained	Predicted	
							CCD	ANN
1	7.5	25	45	30	35	70.6	70.751	70.683
2	7.5	25	45	30	15	55.1	54.422	54.727
3	8.5	15	35	20	25	67.2	67.441	67.333
4	7.5	25	45	30	35	70.6	70.751	70.683
5	6.5	15	55	20	25	64.2	64.233	64.218
6	7.5	5	45	30	35	56.9	57.338	57.141
7	7.5	25	45	30	55	83.1	83.372	83.250
8	7.5	25	45	10	35	60.5	59.988	60.218
9	6.5	35	55	40	25	60.8	61.000	60.910
10	7.5	25	25	30	35	92.8	92.322	92.537
11	8.5	35	35	40	25	54.3	54.708	54.524
12	7.5	25	45	50	35	61.8	61.905	61.858
13	7.5	25	45	30	35	70.7	70.751	70.728
14	7.5	25	65	30	35	82.5	82.572	82.540
15	8.5	15	55	20	45	54.9	54.766	54.826
16	6.5	35	35	20	25	57.1	57.591	57.370
17	6.5	15	35	40	25	48.6	48.616	48.609
18	9.5	25	45	30	35	48.7	48.355	48.510
19	8.5	35	55	40	45	70.3	70.333	70.318
20	6.5	35	55	20	45	54.0	54.116	54.064
21	5.5	25	45	30	35	47.1	47.038	47.066
22	6.5	15	35	20	45	58.5	58.433	58.463
23	8.5	15	35	40	45	62.5	62.350	62.418
24	8.5	15	55	40	25	53.5	53.450	53.473
25	6.5	15	55	40	45	87.9	87.541	87.703
26	7.5	25	45	30	35	70.7	70.751	70.728
27	8.5	35	35	20	45	104.2	104.525	104.379
28	7.5	45	45	30	35	64.5	63.655	64.035
29	6.5	35	35	40	45	75.2	75.300	75.255
30	8.5	35	55	20	25	44.1	44.525	44.334
31	7.5	25	45	30	35	70.7	70.751	70.728
32	7.5	25	45	30	35	70.8	70.751	70.773

Table 4
Analysis of the variance (ANOVA) for the fit of the experimental data to response surface model

Sources	Degree of freedom	Adjusted sum of squares	Adjusted mean squares	F value	P value
Regression	20	5,874.12	293.706	1,035.65	0.000
Linear	5	1,467.71	293.542	1,035.07	0.000
Square	5	1,930.03	386.006	1,361.12	0.000
Interaction	10	2,476.38	247.638	873.21	0.000
Residual error	11	3.12	0.284		
Lack-of-fit	6	3.09	0.515	90.92	0.000
Pure error	5	0.03	0.006	—	—
Total	31	5,877.24	—	—	—

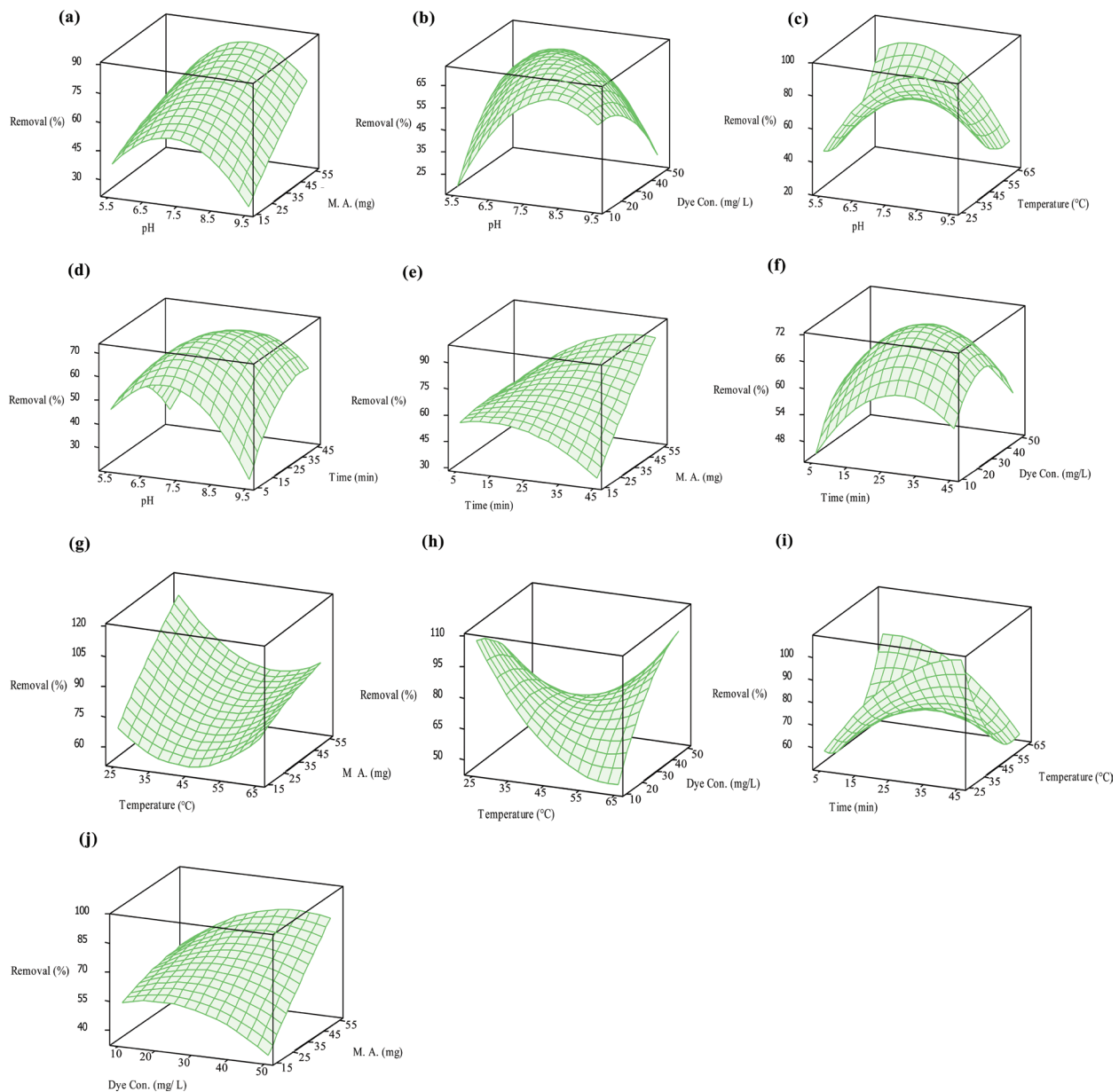


Fig. 4. The surface plots: showing the effect of five interest parameters on the percent of Congo red removal at optimum conditions of 7.12, 25°C, 22.03 min, 16.43 mg L⁻¹, and 48.47 mg, for pH, temperature, time, initial dyes concentration and adsorbent mass.

vice versa. Increasing the temperature results in decrease in the sorptive forces between the active sites on the sorbent and the dye molecules [42]. The effect of temperature was studied in the range of 25°C–65°C. As shown in Fig. 4(c), (g), (h) and (i), by increasing the temperature, a very slight decrease was observed in percent of removal which can be neglected. Therefore, for ease of process, the optimum temperature of 25°C was considered.

4.3.3. The effect of time

One of the most important factors in all chemical processes is reaching to the equilibrium state. In adsorption process, the equilibrium between aqueous solution and

sorbent can noticeably influence the dye removal (%). Consequently, the adsorption time was considered in the range of 5–45 min. As shown in Fig. 4(d), (e) and (f), by increasing the contact time, the removal (%) increases to 22.03 min and remains nearly constant in the range of 22.03–45 min due to the more accomplishment of the adsorption. Hence, the optimum time of 22.03 min was achieved for further studies.

4.3.4. The effect of initial dye concentration and amount of sorbet

The vacant binding sites on the surface of the adsorbent and the concentration of the dye are two important factors that directly the percent of dye removal in the solution.

Therefore, initial dye concentration was considered in the range of 10–50 mg L⁻¹. As the dye concentration increases the active sites saturates the magnetic nano alumina [43]. Fig. 4(b), (f), (h) and (j) show that dye removal percent is almost constant from 10 to 16.43 mg L⁻¹ and up to 16.43 mg L⁻¹ a decreasing trend is observed. Hence, the optimum dye concentration of 10–16.43 mg L⁻¹ was considered for the process. It can be stated that the more the amount of sorbet is the more the vacant and unoccupied sites are on the adsorbent structure to adsorb the dye molecules and also the more contact surface will be provided [30]. The results in Fig. 4(a), (e), (g) and (j) show the dye removal percent has an increasing trend and the optimum sorbet amount of 48.47 mg was selected for the process.

4.4. ANN modeling

The input variables of trained ANN are pH, temperature (Temp.), time, initial dye concentration (Conc.), and amount of magnetic nano alumina (M.A.) and the outputs is adsorption efficiency of Congo red. Fig. 5 represents the topology of ANN in which the number of layers, neurons of each layer and their interconnects are clarified. Table 2 shows the predicted values by ANN. The regression analysis between experimental data and predicted data by ANN showed R^2 value of 0.9998 which represented proper agreements between predicted and experimental responses. The main purpose of ANN training is to obtain the best weights with minimum values of prediction error. The number of neurons in hidden layer, transfer functions and repetition of training step were changed to calculate the minimum prediction error. Several topologies were investigated to obtain the optimum number of neurons in hidden layer, various topologies were considered. The error of each topology is shown in Fig. 6. The ANN with 11 neurons in hidden layer has the minimum value of mean square error (MSE). The most proficient and capable experimental model supplies the minimum MSE. The equation of MSE function is as follows:

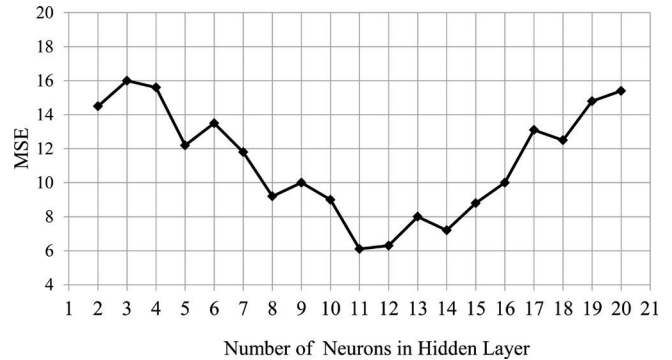


Fig. 6. The mean square error based on variation of neurons in hidden layer.

$$MSE = \frac{1}{N} \sum_{i=1}^N (Y_{pre} - Y_{ex})^2 \quad (8)$$

where Y_{ex} is the experimental output, Y_{pre} is the network output and N is the number of data points [44].

The accuracy of ANN was investigated by using test data set (Table 5). The values of MAPE were acquired 0.2% which reveals high accuracy of the ANN model for process. Fig. 7 represents the MAPE (%) of RSM (CCD) and ANN vs. number of experiments. It is obvious that the MAPE value of RSM model is more than ANN model for each experimental test. Therefore, the accuracy of ANN model is higher than RSM model.

5. Regeneration of adsorbent

The used sorbent can be regenerated by a suitable solvent. To this aim, the polluted sorbent was washed by methanol, ethanol, and acetone. The desorption percent of 60%, 92%, and 65% were obtained at 35°C for methanol, ethanol, and acetone respectively. Therefore, ethanol was chosen as regenerative solvent.

6. Adsorption isotherms

The adsorption isotherm is one of the most important criteria for an adsorption process. The adsorption isotherms refer to the partition of adsorbate molecules between the liquid phase and solid sorbent in the adsorption process. In fact, the adsorption isotherms clarify the relationship between the adsorbent and adsorbate at a specific temperature. The adsorption isotherm indicates information of how much material will adsorb for a known set of state variables. The amount of adsorbed material can be given as surface coverage, i.e., the fraction of occupied/available sites taken up by the sum of particles adsorbed in the first monolayer. In practice, the uptake of adsorptive of a given catalyst material is a decisive quantity, since a high uptake usually means a (desired) high catalyst efficiency. The respective uptake is often called sorption capacity and characterized by the sorption (or adsorption) isotherm. The form of the sorption isotherm provides a lot of first-glance information about the chemical and physical properties of the catalyst

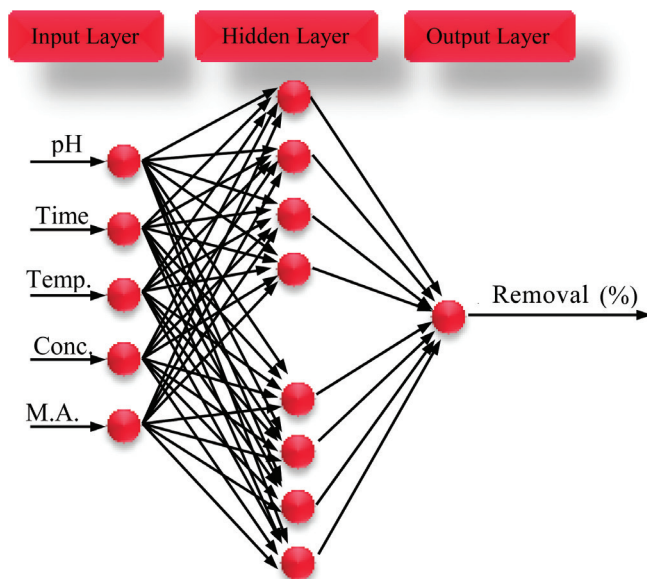


Fig. 5. Optimized topology of artificial neural network.

Table 5
Comparative results of the experiment and predicted values by ANN and CCD for test data set

No.	Factors					Adsorption (%)			APE (%)	
	pH	Time (min)	Temp (°C)	Initial dye con. (mg L ⁻¹)	M.A.C amount (mg)	Exp.	ANN	CCD	ANN	CCD
1	7.5	25	45	30	35	70.6	70.751	0.214	70.683	0.118
2	8.5	35	35	40	25	54.3	54.708	0.751	54.524	0.413
3	6.5	35	35	20	25	57.1	57.591	0.860	57.370	0.473
4	5.5	25	45	30	35	47.1	47.038	0.132	47.066	0.072
5	8.5	15	55	40	25	53.5	53.450	0.093	53.473	0.051
6	6.5	35	35	40	45	75.2	75.300	0.133	75.255	0.073
							MAPE (%)		0.36	0.20

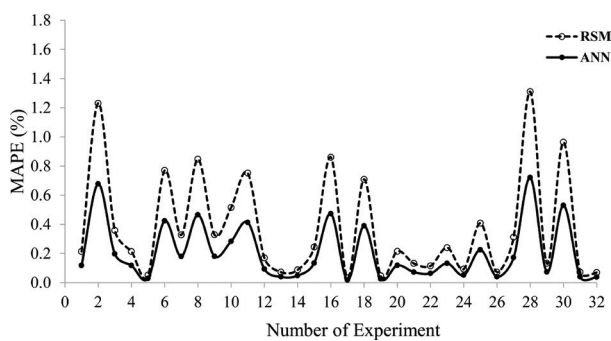


Fig. 7. MAPE (%) of RSM (CCD) and ANN vs. number of experiments.

material and about how the adsorption process proceeds over a given surface. In principle, various kinds of isotherms (such as Linear, Langmuir, Freundlich, and BET) can be distinguished, depending on the nature of the catalyst and the kind of interaction [45]. Therefore, to evaluate the adsorption isotherm of the proposed method, the common isotherms of Langmuir and Freundlich were studied at different concentrations in the range of 5–200 mg L⁻¹ at optimum conditions. Langmuir isotherm has a rational basis and implies the monolayer adsorption on a homogenous adsorbent. As a site is occupied by an ion, no further molecule can be adsorbed at that site [46]. The Langmuir equation is as follows [47]:

$$C_e / Q_e = 1 / (Q_m b) + C_e / Q_m \quad (9)$$

where Q_m is the saturation adsorption capacity (mg g⁻¹) and b the constant related to the free energy of adsorption were obtained from the slope and the intercept of equation. The plots of Q_e vs. C_e and C_e / Q_e vs. C_e are shown in Fig. 8. The favorability of Congo red adsorption onto the magnetic nano alumina can be assessed by dimensionless constant called separation factor, R_L (Eq. (10)).

$$R_L = 1 / (1 + bC_0) \quad (10)$$

In this equation, C_0 (mg g⁻¹) is the highest initial ions concentration in adsorption isotherm studies. The value of R_L implies the unfavorable ($R_L > 1$), linear ($R_L = 1$), favorable ($0 < R_L < 1$), and irreversible ($R_L = 0$) type of the adsorption

isotherm. As the results show in Table 6, the values of R_L for two ions are $0 < R_L < 1$ which are favorable for adsorption isotherm [15, 48].

The Freundlich isotherm is an empirical equation which is commonly applied for many adsorption processes. The Freundlich isotherm was also considered for the process applying Eq. (11) as below:

$$Q_e = K_f C_e^{(1/n)} \quad (11)$$

This can be linearized as follows:

$$\log Q_e = \log K_f + 1/n \log C_e \quad (12)$$

where the K_f is Freundlich constant related to the adsorbent capacity, and n is the constant indicative to the intensity of the adsorption process. The values of the constant n and K_f were calculated from the slope and the intercepts of equation and shown in Table 5. The Langmuir and Freundlich isotherm plots are shown in Fig. 8. The Freundlich intensity constant of Congo red was as $n > 1$ which shows the significant adsorption of Congo red in the proposed procedure even at high ions concentration. The diagrams showed models were ideally fitted to the data of adsorption of Congo red. As it is obvious, Langmuir isotherm plots were obtained by mean correlation coefficient of 0.9138. In addition, Freundlich isotherm was satisfactorily to describe the adsorption of Congo red on magnetic nano alumina.

7. Real sample analysis

The proposed process was carried out on two river water samples which had the possibility and potential of dye pollution due to their closeness to the companies and factories using dye in their industrial processes. As the results show in Table 7, at optimum conditions the prepared sorbent could ideally adsorb Congo red from the industrial samples.

8. Comparison of the maximum adsorption capacity with other studies

Removal Congo red from aqueous solution with magnetic nano alumina was compared with some other studies. As the

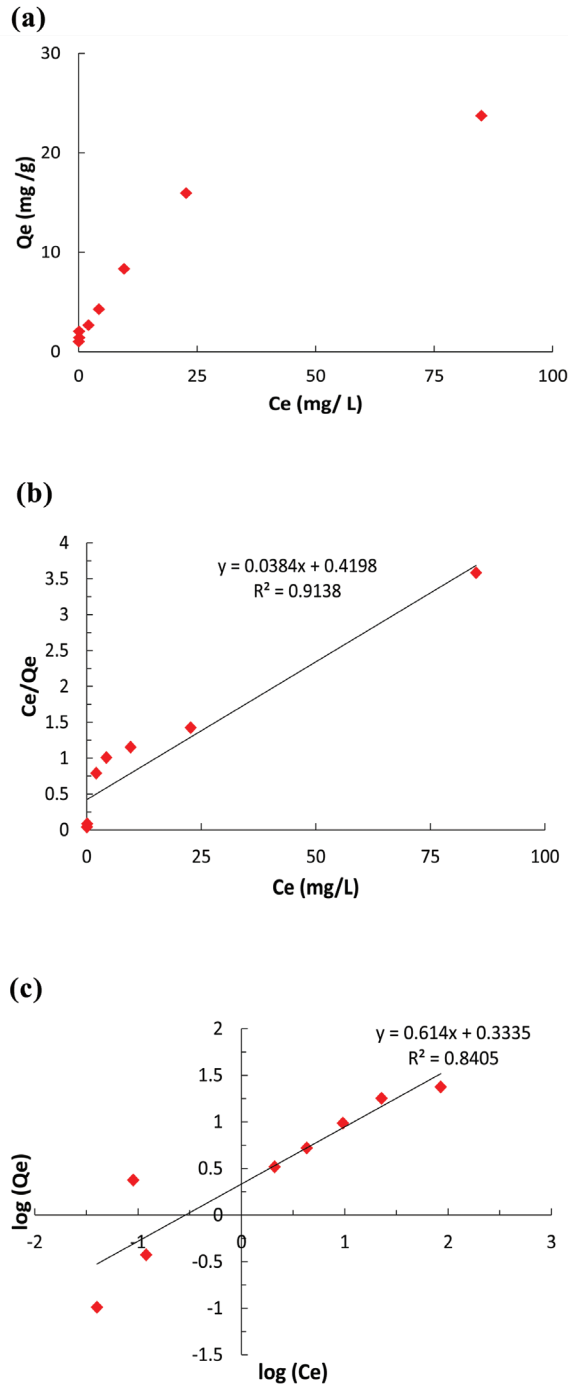


Fig. 8. The adsorption isotherms: (a) Langmuir isotherm plots, (b) Freundlich isotherm plot and (c) obtained at optimum conditions.

Table 6 Isotherm parameters for adsorption of Congo red (CR) onto the magnetic nano alumina at the optimum conditions

Dye	Langmuir isotherm				Freundlich isotherm			
	Q_{max} (mg g ⁻¹)	b (L mg ⁻¹)	R^2	R_L	K_f	1/n	N	R^2
CR	26.0416	0.09148	0.9138	0.0518	2.1552	0.614	1.6286	0.8405

Table 7 Analysis of real sample

Sample	Spiked (mg L ⁻¹)	Measured (mg L ⁻¹)	Removal (%)
Karooon River ^a	0	1.8	—
	5	7.2	102.0
	15	17.0	92.0
Maroon River ^b	0	1.1	—
	5	6.3	96.0
	15	15.9	98.7

^a Karooon river in Ahvaz, Khozestan Province, Iran

^b Maroon river in behbahan, Khozestan Province, Iran

Table 8 Comparison of maximum adsorption capacity of the proposed sorbent with other studies

Sorbent	Q_{max}	Reference
Magnetic alumina	26.04	This study
Apricot stone	23.42	[49]
Banana peel	18.2	[50]
Pineapple (Ananas comosus) plantstem	11.966	[51]
Roots of Eichhornia crassipes	1.58	[52]

results indicated in Table 8, the proposed sorbent has acceptable maximum adsorption capacity of 26.04 mg g⁻¹. Besides the acceptable maximum adsorption capacity of magnetic nano alumina, the facile separation of the magnetic sorbent from the media is the significant advantage of this sorbent.

9. Conclusions

Magnetic nano alumina was prepared and used for removal of Congo red from aqueous solution. The optimum conditions of 7.12, 25°C, 22.03 min, 16.43 mg L⁻¹, and 48.47 mg, for pH, temperature, time, and initial dye concentration, and amount of sorbent were acquired, respectively. The maximum experimentally achieved removal percent of 99.5 ± 0.2 was obtained under optimum conditions which represents the significant potential of the synthesized sorbent. The adsorption isotherms studies indicated favorable fitting of the process in Langmuir and Freundlich isotherms. Two statistical models of RSM and ANN were applied effectively to predict the process with MAPE (%) of 0.36 and 0.20, and the determination coefficient (R^2) of 0.9995 and 0.9998, respectively. The results proved that ANN was more powerful and capable for estimation of the proposed method. Moreover, the proposed

sorbent of magnetic nano alumina utilized in this study can be properly applied in industrial scale due to low-cost sorbent, easy separation and high percent of dye removal.

Acknowledgement

The authors appreciate Shahrekord University and the Center of Excellence for Mathematics, Shahrekord University.

References

- [1] S. Chatterjee, D.S. Lee, M.W. Lee, S.H. Woo, Enhanced adsorption of congo red from aqueous solutions by chitosan hydrogel beads impregnated with cetyl trimethyl ammonium bromide, *Bioresour. Technol.*, 100 (2009) 2803–2809.
- [2] T. Şişmanoğlu, G.S. Pozan, Adsorption of congo red from aqueous solution using various TiO₂ nanoparticles, *Desalin. Water Treat.*, 57 (2016) 13318–13333.
- [3] B. Gözmen, B. Kayan, A.M. Gizir, A. Hesenov, Oxidative degradations of reactive blue 4 dye by different advanced oxidation methods, *J. Hazard. Mater.*, 168 (2009) 129–136.
- [4] D. Morshedi, Z. Mohammadi, M.M. Akbar Boojar, F. Aliakbari, Using protein nanofibrils to remove azo dyes from aqueous solution by the coagulation process, *Colloids Surf. B. Biointerfaces*, 112 (2013) 245–254.
- [5] E. Alventosa-deLara, S. Barredo-Damas, M. Alcaina-Miranda, M. Iborra-Clar, Ultrafiltration technology with a ceramic membrane for reactive dye removal: optimization of membrane performance, *J. Hazard. Mater.*, 209 (2012) 492–500.
- [6] S. Wijannarong, S. Aroonsrimorakot, P. Thavipoke, S. Sangjan, Removal of reactive dyes from textile dyeing industrial effluent by zonation process, *APCBEE Procedia*, 5 (2013) 279–282.
- [7] G.M. Ratnamala, U.B. Deshannavar, S. Munyal, K. Tashildar, S. Patil, A. Shinde, Adsorption of reactive blue dye from aqueous solutions using sawdust as adsorbent: optimization, kinetic, and equilibrium studies, *Arab J. Sci. Eng.*, (2015) 1–12.
- [8] M.H. Dehghani, P. Mahdavi, Removal of acid 4092 dye from aqueous solution by zinc oxide nanoparticles and ultraviolet irradiation, *Desalin. Water Treat.*, 54 (2015) 3464–3469.
- [9] L. Pietrelli, I. Francolini, A. Piozzi, Dyes Adsorption from aqueous solutions by chitosan, *Sep. Sci. Technol.*, 50 (2015) 1101–1107.
- [10] Y. Yu, B.N. Murthy, J.G. Shapter, K.T. Constantopoulos, N.H. Voelcker, A.V. Ellis, Benzene carboxylic acid derivatized graphene oxide nanosheets on natural zeolites as effective adsorbents for cationic dye removal, *J. Hazard. Mater.*, 260 (2013) 330–338.
- [11] V.K. Gupta, B. Gupta, A. Rastogi, S. Agarwal, A. Nayak, A comparative investigation on adsorption performances of mesoporous activated carbon prepared from waste rubber tire and activated carbon for a hazardous azo dye—Acid Blue 113, *J. Hazard. Mater.*, 186 (2011) 891–901.
- [12] V. Srivastava, C.H. Weng, V.K. Singh, Y.C. Sharma, Adsorption of nickel ions from aqueous solutions by nano alumina: kinetic, mass transfer, and equilibrium studies, *J. Chem. Eng. Data*, 56 (2011) 1414–1422.
- [13] A. Bhat, G.B. Megeri, C. Thomas, H. Bhargava, C. Jeevitha, S. Chandrashekar, G.M. Madhu, Adsorption and optimization studies of lead from aqueous solution using γ -Alumina, *J. Environ. Chem. Eng.*, 3 (2015) 30–39.
- [14] J. Zolgharnein, M. Bagtash, T. Shariatmanesh, Simultaneous removal of binary mixture of Brilliant Green and Crystal Violet using derivative spectrophotometric determination, multivariate optimization and adsorption characterization of dyes on surfactant modified nano- γ -alumina, *Spectrochim. Acta, Part A*, 137 (2015) 1016–1028.
- [15] M. Shirani, A. Semnani, H. Haddadi, S. Habibollahi, Optimization of simultaneous removal of methylene blue, crystal violet, and fuchsine from aqueous solutions by magnetic NaY zeolite composite, *Water, Air, Soil Pollut.*, 225 (2014) 1–15.
- [16] S. Shariati, M. Faraji, Y. Yamini, A.A. Rajabi, Fe₃O₄ magnetic nanoparticles modified with sodium dodecyl sulfate for removal of safranin O dye from aqueous solutions, *Desalination*, 270 (2011) 160–165.
- [17] N.M. Mahmoodi, Magnetic ferrite nanoparticle–alginate composite: synthesis, characterization and binary system dye removal, *J. Taiwan Inst. Chem. E*, 44 (2013) 322–330.
- [18] E. Kumar, A. Bhatnagar, U. Kumar, M. Sillanpää, Defluoridation from aqueous solutions by nano-alumina: characterization and sorption studies, *J. Hazard. Mater.*, 186 (2011) 1042–1049.
- [19] D. Bingöl, M. Hecan, S. Elevli, E. Kılıç, Comparison of the results of response surface methodology and artificial neural network for the biosorption of lead using black cumin, *Bioresour. Technol.*, 112 (2012) 111–115.
- [20] F. Amato, A. López, E.M. Peña-Méndez, P. Vañhara, A. Hampl, J. Havel, Artificial neural networks in medical diagnosis, *J. Applied Biomed.*, 11 (2013) 47–58.
- [21] S. Dutta, S.A. Parsons, C. Bhattacharjee, S. Bandhyopadhyay, S. Datta, Development of an artificial neural network model for adsorption and photocatalysis of reactive dye on TiO₂ surface, *Expert Syst. Appl.*, 37 (2010) 8634–8638.
- [22] M. Shirani, A. Akbari, M. Hassani, Adsorption of cadmium(ii) and copper(ii) from soil and water samples onto a magnetic organozeolite modified with 2-(3,4-dihydroxyphenyl)-1,3-dithiane using an artificial neural network and analysed by flame atomic absorption spectrometry, *Anal. Method*, 7 (2015) 6012–6020.
- [23] P. Das, P. Banerjee, A. Zaman, P. Bhattacharya, Biodegradation of two Azo dyes using *Dietzia* sp. PD1: process optimization using Response Surface Methodology and Artificial Neural Network, *Desalin. Water Treat.*, 57 (2016) 7293–7301.
- [24] A. Çelekli, H. Bozkurt, F. Geyik, Artificial neural network and genetic algorithms for modeling of removal of an azo dye on walnut husk, *Desalin. Water Treat.*, (2015) 1–12.
- [25] Y. Yang, G. Wang, B. Wang, Z. Li, X. Jia, Q. Zhou, Y. Zhao, Biosorption of acid black 172 and congo red from aqueous solution by nonviable penicillium YW 01: kinetic study, equilibrium isotherm and artificial neural network modeling, *Bioresour. Technol.*, 102 (2011) 828–834.
- [26] M.A. Bezerra, R.E. Santelli, E.P. Oliveira, L.S. Villar, L.A. Escalera, Response surface methodology (RSM) as a tool for optimization in analytical chemistry, *Talanta*, 76 (2008) 965–977.
- [27] S. Ponnusamy, R. Subramaniam, Process optimization studies of Congo red dye adsorption onto cashew nut shell using response surface methodology, *Int. J. Ind. Chem.*, 4 (2013) 1–10.
- [28] H. Faghianian, M. Moayed, A. Firooz, M. Irvani, Evaluation of a new magnetic zeolite composite for removal of Cs⁺ and Sr²⁺ from aqueous solutions: Kinetic, equilibrium and thermodynamic studies, *Comptes. Rendus. Chimie.*, 17 (2014,) 108–117.
- [29] A.A. Poghossian, Determination of the pH_{pzc} of insulators surface from capacitance–voltage characteristics of MIS and EIS structures, *Sensors Actuators B: Chem.*, 44 (1997) 551–553.
- [30] M.A.M. Salleh, D.K. Mahmoud, W.A.W.A. Karim, A. Idris, Cationic and anionic dye adsorption by agricultural solid wastes: a comprehensive review, *Desalination*, 280 (2011) 1–13.
- [31] B.H. Hameed, I.A.W. Tan, A.L. Ahmad, Adsorption isotherm, kinetic modeling and mechanism of 2,4,6-trichlorophenol on coconut husk-based activated carbon, *Chem. Eng. J.*, 144 (2008) 235–244.
- [32] N. Kannan, T. Veemaraj, Removal of lead (ii) ions by adsorption onto bamboo dust and commercial activated carbons – a comparative study, *J. Chem.*, 6 (2009) 247–256.
- [33] S.S. Prasad, K. Aikat, Optimization of medium for decolorization of Congo red by *Enterobacter* sp. SXCR using response surface methodology, *Desalin. Water Treat.*, 52 (2014) 6166–6174.
- [34] S. Sadaf, H.N. Bhatti, M. Arif, M. Amin, F. Nazar, M. Sultan, Box–Behnken design optimization for the removal of Direct Violet 51 dye from aqueous solution using lignocellulosic waste, *Desalin. Water Treat.*, 56 (2015) 2425–2437.
- [35] E.-C. Khoo, S.-T. Ong, Y.-T. Hung, S.-T. Ha, Removal of basic dyes from aqueous solution using sugarcane bagasse:

- optimization by Plackett–Burman and Response Surface Methodology, *Desalin. Water Treat.*, 51 (2013) 7109–7119.
- [36] S.-T. Ong, E.-C. Khoo, P.-S. Keng, S.-L. Hii, S.-L. Lee, Y.-T. Hung, S.-T. Ha, Plackett–Burman design and response surface methodological approach to optimize basic dyes removal using sugarcane bagasse, *Desalin. Water Treat.*, 25 (2011) 310–318.
- [37] A. Menon, K. Mehrotra, C.K. Mohan, S. Ranka, Characterization of a class of sigmoid functions with applications to neural networks, *Neural Networks*, 9 (1996) 819–835.
- [38] S. Shakeri, A. Ghassemi, M. Hassani, A. Hajian, Investigation of material removal rate and surface roughness in wire electrical discharge machining process for cementation alloy steel using artificial neural network, *Int. J. Adv. Manuf. Technol.*, (2015) 1–9.
- [39] A. Özcan, Ç. Ömeroğlu, Y. Erdoğan, A.S. Özcan, Modification of bentonite with a cationic surfactant: an adsorption study of textile dye Reactive Blue 19, *J. Hazard. Mater.*, 140 (2007) 173–179.
- [40] Y. Önal, C. Akmil-Başar, D. Eren, Ç. Sarıcı-Özdemir, T. Depci, Adsorption kinetics of malachite green onto activated carbon prepared from Tunçbilek lignite, *J. Hazard. Mater.*, 128 (2006) 150–157.
- [41] A.P. Vieira, S.A.A. Santana, C.W.B. Bezerra, H.A.S. Silva, J.A.P. Chaves, J.C.P. de Melo, E.C. da Silva Filho, C. Airoidi, Kinetics and thermodynamics of textile dye adsorption from aqueous solutions using babassu coconut mesocarp, *J. Hazard. Mater.*, 166 (2009) 1272–1278.
- [42] A.E. Ofomaja, Y.-S. Ho, Equilibrium sorption of anionic dye from aqueous solution by palm kernel fibre as sorbent, *Dyes and Pigments*, 74 (2007) 60–66.
- [43] Z. Eren, F.N. Acar, Adsorption of reactive black 5 from an aqueous solution: equilibrium and kinetic studies, *Desalination*, 194 (2006) 1–10.
- [44] S. Elemen, E.P. Akçakoca Kumbasar, S. Yapar, Modeling the adsorption of textile dye on organoclay using an artificial neural network, *Dyes Pigments*, 95 (2012) 102–111.
- [45] K.Y. Foo, B.H. Hameed, Insights into the modeling of adsorption isotherm systems, *Chem. Eng. J.*, 156 (2010) 2–10.
- [46] S. Sohrabnezhad, A. Pourahmad, Comparison adsorption of new methylene blue dye in zeolite and nanocrystal zeolite, *Desalination*, 256 (2010) 84–89.
- [47] H. Faghihian, M. Moayed, A. Firooz, M. Iravani, Synthesis of a novel magnetic zeolite nanocomposite for removal of Cs+ and Sr2+ from aqueous solution: kinetic, equilibrium, and thermodynamic studies, *J. Colloid Interface Sci.*, 393 (2013) 445–451.
- [48] D. Mohan, S. Chander, Single, binary, and multicomponent sorption of iron and manganese on lignite, *J. Colloid Interface Sci.*, 299 (2006) 76–87.
- [49] M. Abbas, M. Trari, Kinetic, equilibrium and thermodynamic study on the removal of Congo Red from aqueous solutions by adsorption onto apricot stone, *Process Saf. Environ. Prot.*, 98 (2015) 424–436.
- [50] G. Annadurai, R.-S. Juang, D.-J. Lee, Use of cellulose-based wastes for adsorption of dyes from aqueous solutions, *J. Hazard. Mater.*, 92 (2002) 263–274.
- [51] S.-L. Chan, Y.P. Tan, A.H. Abdullah, S.-T. Ong, Equilibrium, kinetic and thermodynamic studies of a new potential biosorbent for the removal of Basic Blue 3 and Congo Red dyes: Pineapple (*Ananas comosus*) plant stem, *J. Taiwan Inst. Chem. Eng.*, 61 (2016) 306–315.
- [52] W.C. Wanyonyi, J.M. Onyari, P.M. Shiundu, Adsorption of Congo Red dye from aqueous solutions using roots of *Eichhornia Crassipes*: kinetic and equilibrium studies, *Energy Procedia*, 50 (2014) 862–869.